

# Electrostatic forces and partly hydrogen-free edges of graphene nanoribbons - Supplementary Materials

Sebastian Schneider,<sup>1</sup> Regina Hoffmann-Vogel<sup>2,3\*</sup>

<sup>1</sup>Physikalisches Institut, Karlsruhe Institute of Technology, Wolfgang-Gaede-Str. 1,  
76128 Karlsruhe, Germany.

<sup>2</sup>Department of Physics, University of Konstanz, Universitätsstrasse 10, 78464 Konstanz,  
Konstanz, Germany.

<sup>3</sup>Institut für Physik und Astronomie, Universität Potsdam, Karl-  
Liebknecht-Str. 24-25, 14476 Potsdam, Germany.

\*Correspondence to: hoffmannvogel@uni-potsdam.de.

## **1 On-surface synthesis of graphene nanoribbons from DBBA oligomers and images obtained at room temperature**

On-surface synthesis of the graphene nanoribbons from 10,10'-dibromo-9,9'-bianthryl (DBBA) (ref (1–3)) relies on the formation of DBBA oligomers. In the DBBA oligomers there are still hydrogen atoms present protecting the oligomers from forming graphene nanoribbons. Further heating allows to remove the hydrogen atoms and form graphene nanoribbons.

Large-amplitude scanning force microscopy images (Fig. S1) show a clear height difference between DBBA oligomers and graphene nanoribbons - demonstrating that the final synthesis step where the hydrogen atoms are removed from the DBBA oligomer is successful. DBBA oligomers are detected from their increased height, from the zigzag shape of the alternating

anthracene units and from the period of their zigzag structure whereas the graphene nanoribbons show no internal structure in standard large-amplitude scanning force microscopy images. The width (0.14 nm) and height (0.19 nm) of the graphene nanoribbons can be measured from the line profile (Fig. S1D) and compared to the height of a DBBA oligomer (0.30 nm). For other measurements, the height of graphene nanoribbons appears even smaller (0.8 nm). The period of the zigzag structure observed on the DBBA oligomers is expected to be approximately 0.85 nm - twice the value measured for the internal structure of graphene nanoribbons.

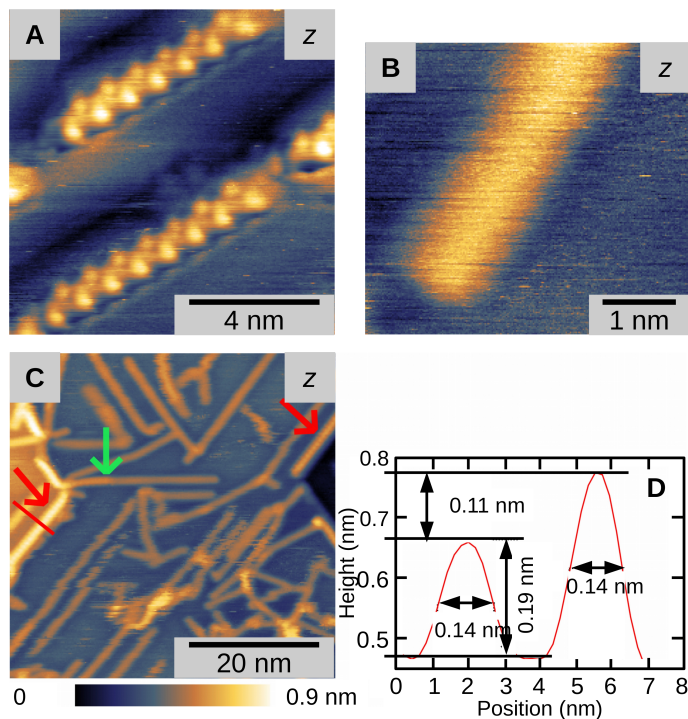


**Fig. S1: Images using standard large-amplitude cantilever SFM.** (A) Image of a DBBA oligomer. The DBBA oligomers clearly show a zigzag internal structure easily resolved by SFM. The period is approximately 1 nm in this image.  $\Delta f = -27$  Hz,  $A = 8$  nm,  $c_L = 43$  N/m,  $f_1 = 351$  kHz. (B) Image of a graphene nanoribbon. (C) Overview image showing graphene nanoribbons on a Au(111) surface after on-surface synthesis. The red arrows show

DBBA oligomers. The green arrow shows a junction between a graphene nanoribbon and a DBBA oligomer. The profile shown in B is taken at the position of the red line. **(D)** Profile along the red line in C showing a direct comparison of a DBBA oligomer with a graphene nanoribbon. The DBBA oligomer is 0.11 nm higher than the graphene nanoribbon.  $\Delta f = -29$  Hz,  $A = 7$  nm,  $c_L = 40$  N/m,  $f_1 = 340$  kHz.

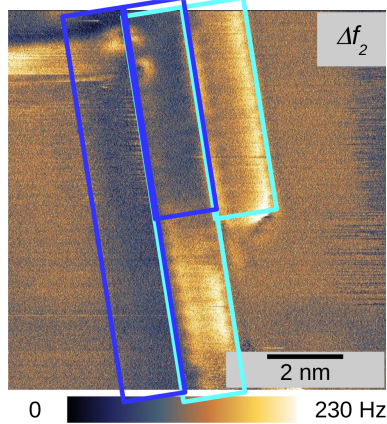


**Fig. S2: Indication of the shadow of the two nanoribbons depicted in dark blue.** The two dark blue rectangles are the same as the two light blue rectangles indicating the brighter graphene nanoribbons.

## 2 Tip shape and termination

In Figure 2a of the main text, a bright shadow is observed next to the two adjacent nanoribbons and has been marked by red arrows. This shadow in Figure 2A corresponds to a darker region at the same position relative to the nanoribbons in Figure 2B. The darker area is about 35 Hz lower in frequency shift compared to the adjacent Au terrace translating to a distance of 62 pm. The size and shape of the shadow is similar in forward and backward scans and remains similar when changing the scanning speed. Figures 2 and 3 have been acquired using different scanning speeds while maintaining the same image size.

The size and shape of the shadow is precisely that of the longer graphene nanoribbon observed in the center of the image and adjacent to the right hand side of the shadow. In addition, there is a shadow overlaid on the upper part of the graphene nanoribbon located at the left hand side also about 35 Hz lower compared to the brighter part of the nanoribbon. This shadow has precisely the shape of the shorter graphene nanoribbon observed on the right hand side of the

image and adjacent to the right hand side of the shadow. We indicate the two shadows by two dark blue rectangles on Figure S2. The shorter nanoribbon appears somewhat wider than the longer one and its edge covers the edge of the longer nanoribbon. Maintaining the same distance between the two light blue rectangles and moving them sideways by precisely the width of one graphene nanoribbon generates the two dark blue rectangles in registry with the shadow.

These observations point to a double tip where the distance of the two tips is precisely the width of a graphene nanoribbon. Since the two edges of the graphene nanoribbons give the strongest interaction, we argue that a graphene nanoribbon has been adsorbed to the tip, see model in Figure S3. In this model, for the tip we have assumed a radius of 2 nm in accordance to the values given by the manufacturer and in agreement to a quantitative description of long-range electrostatic forces in scanning force microscopy measurements, as has been given e.g. in ref (4). One of the corners of the graphene nanoribbon gives the strongest tip-sample interaction and generates the main image. The other corner is located at a slightly larger distance from the sample surface and merely generates a dark shadow overlaid to the main image.

We can even determine the orientation of the graphene nanoribbon. Since the shadow next to the graphene nanoribbons on the surface has precisely the width of a graphene nanoribbon, the graphene nanoribbon on the tip must be oriented parallel to the graphene nanoribbons on the surface in this image. In this configuration it exposes a zigzag edge to the sample. One of the two corners of the zigzag edge gives a brighter image, because the zigzag edge is tilted with respect to the surface. In this configuration one corner of the zigzag edge forms the tip apex.

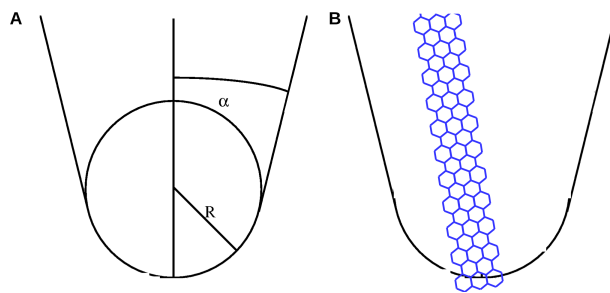


**Fig. S3: Model of the tip.** (A) Usually the manufacturer supplies an opening angle and a tip radius. (B) We assume a tip radius of 2 nm, the nanoribbon, depicted in blue, has a width of about 1 nm and a thickness of several Å.

### **3 Bright edges of graphene nanoribbons observed through tip change at 115 K**

In the main article we discuss how bimodal mode enhances the contrast at the edges of the graphene nanoribbons and the sensitivity of the measurement to long-range electrostatic forces. In these measurements, the contrast in the fundamental mode topography images remains as well-known for graphene nanoribbons. In this section, we show images obtained in monomode dynamic frequency modulation scanning force microscopy images where the contrast has changed by a tip change. In these images in the topography channel the edges also look bright. In these measurements the tip has been cleaned by Ar ion sputtering.

To obtain the images shown here, first we imaged a region containing graphene nanoribbons using scanning force microscopy (Fig. S4A). Then a disordered region of the surface was imaged using the same tip. Subsequently, we imaged again the same region containing graphene nanoribbons as before. The tip has changed (Fig. S4B) and after the tip change bright contrast is observed on the edges of the graphene nanoribbons. When we took another image at the same area, the tip had changed back to its original state (Fig. S4C). For Figure S4B we have no indications that a graphene nanoribbon could have been adsorbed to the tip.

We compare these measurements to Fig. 3A of the main text. In the two different measurements the tip-sample distance could differ and the relative importance of different types of forces could be different. In particular the role of the chemical interaction should strongly depend on the chemical details of the tip apex. It is remarkable that in Fig. S4B the interaction of the tip and the graphene nanoribbon's edge is attractive in contrast to Fig. 3A of the main text where the interaction is repulsive. This could give additional information on the nature of the tip and on contrast formation in these measurements. The partial charge of the tip used here in Fig. S4B could be opposite to the one on the graphene nanoribbon's edge to explain the

difference.

On the right hand side of Figure S4B two areas with dark edges have been marked with white arrows. These areas are defective and the graphene nanoribbon could be hydrogen-terminated at these areas similar to the defect shown in the main text.

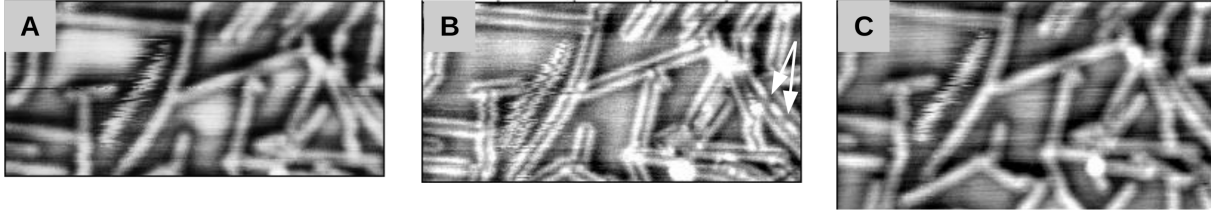


**Fig. S4: Sequence of images showing a tip change and bright edge contrast.** These images were obtained in standard frequency modulation scanning force microscopy mode with the bimodal oscillation switched off. They show the sample topography at constant frequency shift. (A) Image obtained on graphene nanoribbons. (B) After a tip change, the edges of the nanoribbons show bright contrast. (C) The contrast changes back to its original state in the subsequent image.  $c_L = 37$  N/m,  $f_0 = 331$  Hz,  $\Delta f = -16$  Hz,  $A = 6$  nm,  $Q = 24000$  and  $T = 115$  K.

## References

1. J. Cai, *et al.*, *Nature* **446**, 470 (2010).
2. S. Schneider, Herstellung von graphenstreifen und ihre untersuchung mit rasterkraftmikroskopie, Ph.D. thesis, Karlsruhe Institute of Technology (2016).
3. K. Bytyqi, Untersuchung von DBBA auf der Au(111)-oberfläche als vorstufe zur herstellung von graphen-nanostreifen, Ph.D. thesis, Karlsruhe Institute of Technology (2015).
4. M. A. Lantz, *et al.*, *Phys. Rev. B* **68**, 035324 (2003).